Acta Pharmacologica Sinica (2017) 38: 331–341
 1671-4083/17
www.nature.com/aps

Original Article

Luteolin-7-diglucuronide attenuates isoproterenol-induced myocardial injury and fibrosis in mice

Bing-bing NING[1, #], Yong ZHANG[2, #], Dan-dan WU[1], Jin-gang CUI[1], Li LIU[1], Pei-wei WANG[1], Wen-jian WANG[1], Wei-liang ZHU[2], Yu CHEN[1, *], Teng ZHANG[1, *]

[1]*Clinical Research Institute of Integrative Medicine, Yueyang Hospital, Shanghai University of Traditional Chinese Medicine, Shanghai 200437, China;* [2]*Shanghai Institute of Materia Medica, Chinese Academy of Sciences, Shanghai 201203, China*

Abstract

Myocardial injury and ensuing fibrotic alterations impair normal heart architecture and cause cardiac dysfunction. Oxidative stress has been recognized as a key player in the pathogenesis of cardiac injury and progression of cardiac dysfunction, and promoting fibrosis. In the current study we investigated whether luteolin-7-diglucuronide (L7DG), a naturally occurring antioxidant found in edible plants, could attenuate isoproterenol (ISO)-induced myocardial injury and fibrosis in mice and the underlying mechanisms. Myocardial injury and fibrosis were induced in mice via injection of ISO (5 mg·kg^{-1}·d^{-1}, ip) for 5 or 10 d. Two treatment regimens (pretreatment and posttreatment) were employed to administer L7DG (5–40 mg·kg^{-1}·d^{-1}, ip) into the mice. After the mice were euthanized, morphological examinations of heart sections revealed that both L7DG pretreatment and posttreatment regimens significantly attenuated ISO-induced myocardial injury and fibrosis. But the pretreatment regimen caused better protection against ISO-induced myocardial fibrosis than the posttreatment regimen. Furthermore, L7DG pretreatment blocked ISO-stimulated expression of the genes (Cyba, Cybb, Ncf1, Ncf4 and Rac2) encoding the enzymatic subunits of NADPH oxidase, which was the primary source of oxidant production in mammalian cells. Moreover, L7DG pretreatment significantly suppressed ISO-stimulated expression of collagen genes Col1a1, Col1a2, Col3a1, and Col12a1 and non-collagen extracellular matrix genes fibrillin-1, elastin, collagen triple helix repeat containing 1 and connective tissue growth factor. In addition, L7DG pretreatment almost reversed ISO-altered expression of microRNAs that were crosstalking with TGFβ-mediated fibrosis, including miR-29c-3p, miR-29c-5p, miR-30c-3p, miR-30c-5p and miR-21. The current study demonstrated for the first time that L7DG is pharmacologically effective in protecting the heart against developing ISO-induced injury and fibrosis, justifying further evaluation of L7DG as a cardioprotective agent to treat related cardiovascular diseases.

Keywords: luteolin-7-diglucuronide; ISO; myocardial injury; myocardial fibrosis; NADPH oxidase; collagen genes; microRNAs; TGFβ

Acta Pharmacologica Sinica (2017) 38: 331–341; doi: 10.1038/aps.2016.142; published online 16 Jan 2017

Introduction

Myocardial fibrosis is a commonly encountered pathology of the failing heart resulting from various injuries to the heart and eventually leads to the destruction of normal tissue architecture and progressive dysfunction in the heart[1, 2]. Clinical studies have also indicated that fibrosis is an independent predictive factor of adverse cardiac outcomes[3–5]. Therapies alleviating myocardial fibrosis remain to be developed for effective cardiac protection.

Tightly regulated and low levels of reactive oxygen species (ROS) are required for normal cellular function. However, excess production of ROS during oxidative stress can damage macromolecules and trigger cell death. Oxidative stress has been recognized as a key player in the pathogenesis of cardiac injury and progression of cardiac dysfunction under a variety of pathological conditions; promoting fibrosis by exacerbating the inflammatory response in addition to modulating collagen synthesis[6]. NADPH oxidase, a multisubunit enzymatic complex, is the primary source of oxidant generation in mammalian cells[7]. NADPH oxidase consists of membrane-associated gp91^{phox} encoded by Cybb and p22^{phox} encoded by Cyba, as well as cytosolic subunits, including p47^{phox} encoded by Ncf1, p67^{phox} encoded by Ncf2, p40^{phox} encoded by Ncf4 and Rac2. Activated NADPH oxidase mediates the production of the ROS precursor, superoxide anion. NADPH oxidase-mediated ROS generation has been shown to play an important role in the pathogenesis of myocardial infarction[8]. Our previous study also demonstrated that pharmacological inhibition of NADPH oxidase-mediated ROS generation prevents the

# These authors contributed equally to this work.
*To whom correspondence should be addressed.
E-mail zhangteng501@hotmail.com (Teng ZHANG);
chenyu6639@hotmail.com (Yu CHEN)
Received 2016-06-17 Accepted 2016-11-07

development of myocardial injury and cardiac fibrogenesis in mouse[9].

Fibrosis is initiated by cytokines and growth factors produced by activated macrophages and inflammatory cells during the inflammatory phase following tissue injury, followed by the activation of fibroblasts and excessive matrix deposition, including the accumulation of collagen and non-collagen extracellular matrix (ECM) gene products. Transforming growth factor β (TGFβ) is the major regulator in the fibrogenic processes. TGFβ induces the expression of various ECM genes in myofibroblasts playing critical roles in promoting fibrogenesis[10].

microRNAs (miRNAs) are short non-coding RNAs that are 21 to 25 nucleotides in length. miRNAs bind to target mRNA molecules and negatively regulate gene expression in various manners, including mRNA cleavage, deadenylation, and translational repression[11]. miRNAs usually modulate the expression of multiple genes in related functional pathways, thus fine-tuning the activity of involved pathways. Extensive studies have revealed that miRNA-mediated gene regulation is mechanistically implicated in virtually all cellular and pathophysiological processes[12]. It has been demonstrated that miRNAs regulating ECM genes also crosstalk with TGFβ1 signaling during fibrogenesis[13].

Luteolin 7-*O*-[*β*-glucuronosyl(1→2) *β*-glucuronide] (luteolin-7-diglucuronide, L7DG) is a naturally occurring flavonoid glycoside found in leaves of basil or *Verbena officinalis* L. It has been reported to possess antioxidant and antifungal activities *in vitro*[14]. It has also been reported to inhibit the proliferation of murine mesangial cells *in vitro*[15]. However, little is known about the pharmacological effect of L7DG *in vivo*. Isoproterenol (ISO), a sympathomimetic β-adrenergic receptor agonist, induces infarcts, such as cardiac muscle cell death. The animal model of ISO-induced myocardial injury recapitulates major metabolic and morphological changes that occur during human myocardial infarction, thus being widely adopted as an experimental model to evaluate cardioprotective effects of pharmacological agents[16–21].

In the current study, L7DG was for the first time isolated from long tube ground ivy (*Glechoma longituba* (Nakai) Kupr), a vegetable plant with medicinal properties. After structural identification and purification, L7DG was further examined for its effects on ISO-induced myocardial injury and fibrotic changes in mouse via histological and molecular biological approaches. The impact of L7DG on the miRNAs involved in fibrosis was also investigated. The results demonstrated preventive and therapeutic effects of L7DG treatment on alleviating the histological manifestations of ISO-induced myocardial injury and fibrosis. L7DG pretreatment also counteracted the aberrant expression of genes encoding NADPH oxidase, collagen and non-collagen ECM genes and miRNAs implicated in tissue fibrosis in ISO-challenged mouse hearts.

Materials and methods

Isolation and structural identification of L7DG

The whole plant of *Glechoma longituba* (Nakai) Kupr (100 g) was air-dried and reflux-extracted twice with H_2O (1 L) at 100 °C (1.5 h each time). The solvent was then evaporated under reduced pressure to 200 mL. The concentrated solution was subsequently treated with 600 mL of 100% ethanol (EtOH) to separate the supernatant from the precipitate. The precipitate was dissolved in 100 mL of water, applied to a D101 column (8.0 cm×80 cm) (Resin D101, Sinopharm Chemical Reagent Co, Ltd, China), and eluted in a stepwise manner by H_2O, 15% EtOH, 60% EtOH and 100% EtOH, each in a volume of 1 L. The 15% EtOH elute was concentrated and separated by ODS-A column (2.0 cm×40 cm) (YMC GEL ODS-A-HG (S-50 μm), Japan) chromatography (0%–100%, MeOH-H_2O) to yield L7DG (136.6 mg). The purity of L7DG (tR=7.1 min, purity >98%) was assessed by HPLC (Agilent ZORBAX SB-C_{18}, 5 μm, 4.6 mm×250 mm, flow rate: 1.0 mL/min) eluted with ACN/0.2% HAc (15:85). The structure of L7DG was identified by spectral evidence, which included ESI-MS, NMR, and UV analyses. ESI-MS *m/z*: 637 $[M-H]^-$; ESI-MS *m/z*: 639 $[M+H]^+$. ^{1}H NMR (DMSO+D_2O, 400 MHz) δ: 7.47 (2H, *d*, J=1.9 Hz, H-2′), 7.43 (1H, dd, J=8.2, 1.9 Hz, H-6′), 6.96 (1H, *s*, H-3), 6.89 (1H, *d*, J=8.2 Hz, H-5′), 6.71 (1H, *d*, J=2.2 Hz, H-8), 6.49 (1H, *d*, J=2.2 Hz, H-6), 5.20 (1H, *d*, J=6.5 Hz, H-1″), 4.57 (1H, *d*, J=6.3 Hz, H-1‴), 3.20–4.1 (*m*, hidden). ^{13}C NMR (DMSO-d6+D_2O, 100 MHz) δ: 182.4 (C-4), 172.9 (C-6‴), 170.2 (C-6″), 164.9 (C-2), 163.2 (C-7), 161.0 (C-9), 157.2 (C-5), 150.1 (C-4′), 146.0 (C-3′), 121.7 (C-1′), 119.6 (C-6′), 116.5 (C-5′), 113.7 (C-2′), 105.8 (C-1‴), 104.0 (C-10), 103.4 (C-3), 100.3 (C-6), 98.5 (C-1″), 96.2 (C-8), 81.8 (C-2″), 76.2 (C-5‴), 75.8 (C-3‴), 75.1 (C-5″), 74.6 (C-3″), 74.4 (C-2‴), 72.2 (C-4″), 71.6 (C-4‴). The structure, purity and UV spectrum of L7DG are shown in Figure 1.

Animals and treatment

Six-week-old C57BL/6J mice were obtained from the Shanghai Laboratory Animal Research Center. Mice were maintained on regular chow *ad libitum*. All the animal handling procedures were approved by the Institutional Animal Care and Use Committee of Shanghai University of TCM. Two treatment regimens, namely pretreatment and posttreatment regimens, were used to assess the effect of L7DG. For the pretreatment regimen (Supplemental Figure 1A), ISO (Sigma-Aldrich, USA) dissolved in PBS was intraperitoneally administered to mice at the dose of 5 mg/kg body weight (bw) once daily for 5 d to induce myocardial injury. L7DG was dissolved in 0.9% saline and intraperitoneally injected into mice 30 min prior to each ISO administration. The dose of L7DG examined included 5, 10, 20, and 40 mg/kg bw. The mice were euthanized on d 6. For the posttreatment regimen (Figure S1B), daily ISO administration at 5 mg/kg bw was delivered in the same manner as mentioned above for 10 d. Starting from d 6 after initiation of ISO challenge, L7DG was administered at the dose of 40 mg/kg bw along with vehicle treatment for the remaining 5 d. The mice were euthanized on d 11. Sterile PBS and 0.9% saline were included as vehicle controls for ISO and L7DG, respectively.

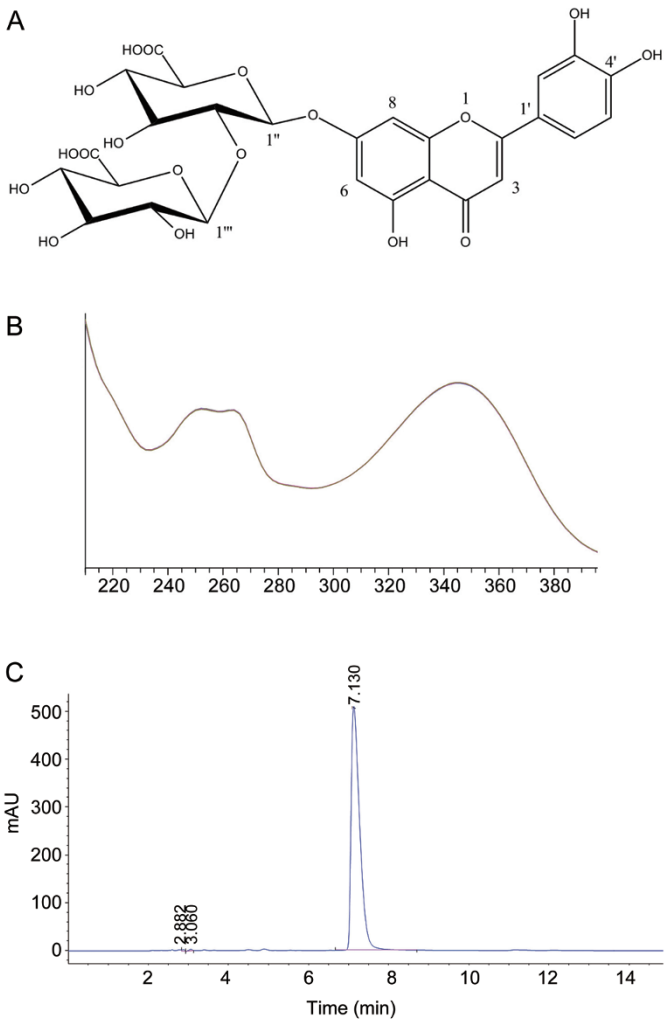

Figure 1. The structure and purity of L7DG. L7DG was isolated from the whole plant of *G longituba* (Nakai) Kupr. (A) The structure of L7DG. (B) The UV spectrum of L7DG. (C) HPLC analysis of the purity of LC1 (t_R=7.1 min, purity >98%).

Histological examination

Mice were euthanized at the end of the experiment, and the hearts were dissected and fixed in 4% paraformaldehyde prior to further processing. For the histological examination of mouse hearts, paraffin sections 5-μm thick were prepared and subjected to hematoxylin and eosin (H&E), Masson's trichrome and Picrosirius red staining. Grading of H&E-stained sections was performed based on the criteria indicated below. Grade 0 (–): no myocardial necrosis, granulation, inflammatory cell infiltration; Grade 1 (+/–): sporadic and isolated myocardial necrotic injury; Grade 2 (+): merged myocardial injuries occurring in less than 30% of the subendocardium; Grade 3 (++): extensive myocardial injuries occurring in more than 30% and less than 50% of the subendocardium; and Grade 4 (+++): extensive myocardial injuries occurring in more than 50% of the subendocardium.

Immunohistochemistry (IHC)

Heart cryosections 10-μm thick were made and subjected to IHC examination to assess the expression of indicated proteins using primary antibodies against α-smooth muscle actin (α-SMA) (Sigma, USA), 4-hydroxynonenal (4-HNE, Abcam, UK), TGFβ1 and phosphorylated-Smad2 (p-Smad2) (Protein Tech, China). Goat-anti-mouse IgG (Solarbio, China) was used to detect α-SMA, goat-anti-mouse IgG-FITC (Solarbio, China) was used to detect 4-HNE, and goat-anti-rabbit IgG (Solarbio, China) was used to detect TGFβ1 and p-Smad2. The immunoreactivity of α-SMA, TGFβ1 and p-Smad2 was developed using diaminobenzidine (Sigma, USA) and observed and recorded using a light microscope (Leica, Germany). The immunoreactivity of 4-HNE was observed using a fluorescence microscope (Leica, Germany).

Real-time PCR analysis

For gene expression analysis, total RNA was isolated and purified using the miRNeasy Mini Kit (Qiagen, USA) and reverse-transcribed using the RevertAid First Strand cDNA Synthesis kit (Thermo, USA). For miRNA expression analysis, total RNA was extracted from paraffin-embedded heart sections using the RecoverAll Total Nucleic Acid Isolation kit (Life Technologies, USA) and reverse-transcribed using the miScript Reverse Transcription Kit (QIAGEN, Germany). Primer sequences for gene expression and miRNA expression analyses are listed in Table 1. Real-time PCR reactions were carried out using the miScript SYBR Green PCR kit (QIAGEN,

Table 1. Primer sequences.

Primers	Forward primer (5'–3')	Reverse primer (5'–3')
Rac2	AAGAAGCTGGCTCCCATCAC	GGTGACACCCCTAGAGCAGG
Cyba	CCTCCACTTCCTGTTGTCGG	ATGGCTGCCAGCAGATAGAT
Cybb	GGGAACTGGGCTGTGAATGA	CAGTGCTGACCCAAGGAGTT
Ncf1	GTTGGGTCCCTGCATCCTAT	ACCAGCCATCCAGGAGCTTA
Ncf2	AGGCTACAGACTAGTGAACTCAT	GGTCTGAGCTTACTTCAAGGGA
Ncf4	GGAAGTGAGAGGTGAACTCGG	AAAGTCGCTCTCTGATCGCA
Col1a1	ACGCCATCAAGGTCTACTGC	ACTCGAACGGGAATCCATCG
Col1a2	AGTCGATGGCTGCTCCAAAA	AGCACCACCAATGTCCAGAG
Col3a1	TGACTGTCCCACGTAAGCAC	GAGGGCCATAGCTGAACTGA
Col12a1	GCTATCCAGGTTCCGGCTAA	TGCCGCGAGATTTCCATACA
Elastin	GCTGATCCTCTTGCTCAACCT	AAGTCCGGCACCTGGCTTAG
Fbn1	AGAGTTGGGGCAGAGACTGT	GTCCCTGCCTGTCTGGACTA
CTGF	CCCGAGTTACCAATGACAATACCT	GGCTTGGCGATTTTAGGTGTC
α-SMA	AGCCATCTTTCATTGGGATGG	CCCCTGACAGGACGTTGTTA
TGFβ1	AGCTGCGCTTGCAGAGATTA	AGCCCTGTATTCCGTCTCCT
TGFβRI	TGAATCCTTCAAACGCGCTG	TGGCCTTAACTTCTGTTCGCA
CTHRC1	ATCCCAGGTCGGGATGGATT	CGTGAATGTACACTCCGCAA
miR-21	CGTAGCTTATCAGACTGATGTTGA	Universal primer
miR-29c-3p	TAGCACCATTTGAAATCGGTTA	Universal primer
miR-29c-5p	ACCGATTTCTCCTGGTGTTC	Universal primer
miR-30c-5p	TGTAAACATCCTACACTCTCAGC	Universal primer
miR-30c-1-3p	TGGGAGAGGGTTGTTTACTCC	Universal primer
miR-24	TGGCTCAGTTCAGCAGGA	Universal primer

Germany) on Light Cycler 480 II (Roche Diagnostics Ltd, Switzerland).

Statistical analysis

The results were averaged from at least three independent experiments, and the data are expressed as the mean±SEM. The Wilcoxon rank-sum test was used for the statistical analyses of histological grading of myocardial injuries, and independent samples *t*-test (SPSS 18, USA) was used for the remaining statistical analyses with *P* values less than 0.05 being considered statistically significant.

Results

L7DG prevents the development of ISO-induced myocardial injury in mouse

L7DG has been indicated as an antioxidant *in vitro*[14]. Oxidative stress is mechanistically involved in the pathogenesis of ISO-induced myocardial injury[9, 21]. To further assess the pharmacological implication of L7DG *in vivo*, the putative effect of L7DG on ISO-induced myocardial injury was examined by a pretreatment regimen (Figure S1A). L7DG was administered at the indicated doses to ISO-challenged mice. As shown in Figure 2 and Table 2, morphological examination of heart sections by H&E staining revealed that compared to the normal morphology exhibited by vehicle-treated normal controls, necrotic degeneration, granulation and inflammatory cell infiltration were readily detected in ISO-challenged vehicle-treated hearts. L7DG pretreatment, however, resulted in dose-dependent protection against ISO-induced myocardial injury. No protection was observed in ISO-challenged mice treated with L7DG at 5 mg/kg bw. Significant protection was observed in ISO-challenged mice treated with L7DG at 20 and 40 mg/kg bw. The preventive effects of L7DG against ISO-induced myocardial injury were reproducibly observed in an independently repeated experiment. As shown in Supplemental Figure 2 and Supplemental Table 1, in distinct contrast to those manifested by ISO-challenged vehicle-treated mice, no overt pathologies indicative of myocardial injury were observed in the heart sections of ISO-challenged mice pretreated with L7DG at 40 mg/kg bw. These results indicate that L7DG pretreatment prevents mice from developing ISO-induced myocardial injury.

Table 2. L7DG protected the hearts against ISO-induced myocardial injury.

Group	Histopathology score					
	–	+–	+	++	+++	*P* value
VC	5					
ISO			1	3	2	0.004
L7DG-5 mg/kg			1	2	1	0.728
L7DG-10 mg/kg		1	2	1		0.057
L7DG-20 mg/kg	1	2	1			0.009
L7DG-40 mg/kg	3	1				0.007

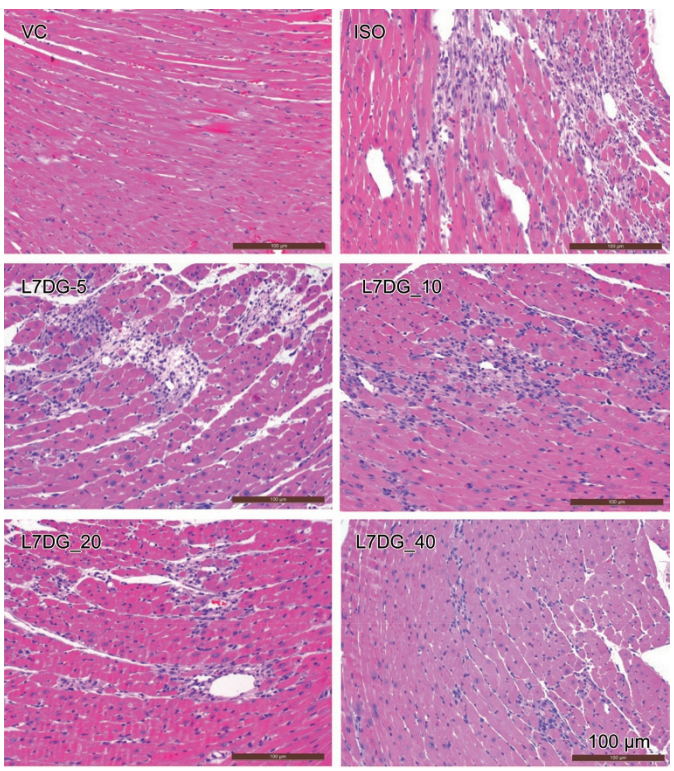

Figure 2. L7DG1 pretreatment prevented the mouse heart from developing ISO-induced myocardial injury. Hearts were collected from vehicle-treated normal controls (VC), ISO-challenged and vehicle-treated mice (ISO), and ISO-challenged mice treated with L7DG at 5 mg/kg bw (L7DG_5), 10 mg/kg bw (L7DG_10), 20 mg/kg bw (L7DG_20), and 40 mg/kg bw (L7DG_40). H&E staining was performed to assess the gross histology of the heart (n=4–6 per group). Scale bar: 100 μm.

L7DG pretreatment suppresses ISO-induced oxidative stress and upregulation of NADPH oxidase

Given that L7DG has been indicated as a natural antioxidant *in vitro*[14], oxidative stress was examined in the absence or presence of L7DG pretreatment. As shown in Figure S3, the immunoreactivity of 4-HNE, a product of lipid peroxidation during oxidative stress, was readily detected in the heart sections of ISO-challenged vehicle-treated mice. In contrast, the immunoreactivity of 4-HNE was barely observed in the heart sections of ISO-challenged mice pretreated with L7DG at 40 mg/kg bw, exhibiting similar patterns as those from vehicle-treated normal controls. Moreover, as NADPH oxidase-mediated oxidant generation is mechanistically implicated in the pathogenesis of myocardial injury and fibrotic disorders, including ISO-induced myocardial injury[8, 9, 22], the possible impact of L7DG on the expression of NADPH oxidase subunits in ISO-induced myocardial injury was further examined. As shown in Figure 3, compared to that from vehicle-treated normal controls, except for Ncf2, significantly increased expression of NADPH oxidase subunits Cyba, Cybb, Ncf1, Ncf4, and Rac2 was observed in the hearts of ISO-challenged vehicle-treated mice. In contrast, significantly downregulated expression of Cyba, Cybb, Ncf1, Ncf4, and Rac2 was found

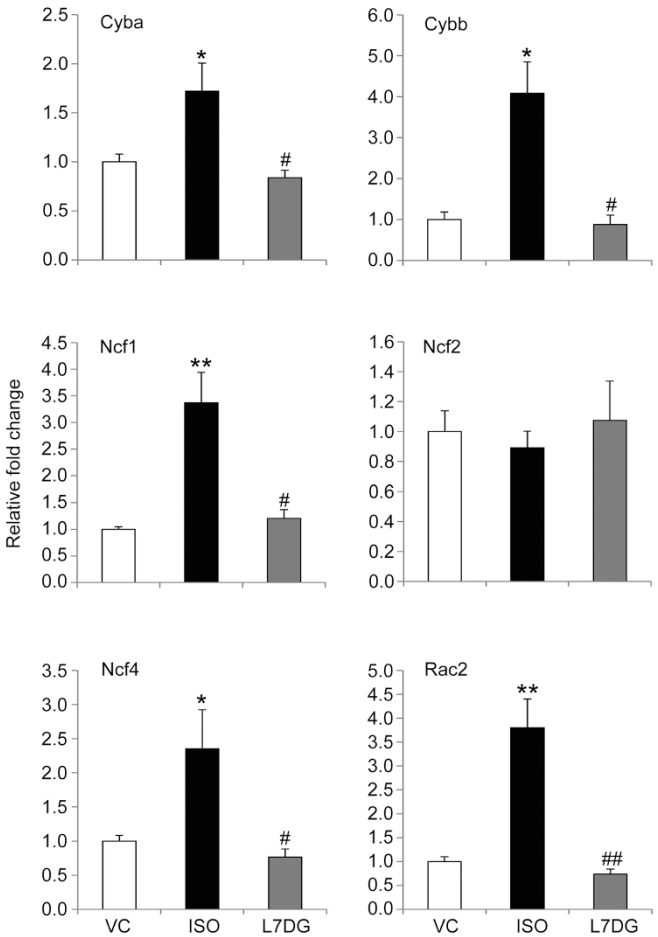

Figure 3. L7DG pretreatment decreased the expression of genes encoding NADPH oxidase. Total RNA was isolated from the hearts collected from vehicle-treated normal controls (VC), ISO-challenged vehicle-treated mice (ISO), and ISO-challenged mice pretreated with L7DG at 40 mg/kg bw (L7DG). Real-time PCR was then performed to analyze the relative expression of genes, including Cyba, Cybb, Ncf1, Ncf2, Ncf4, and Rac2. The relative fold change in gene expression was plotted against that of the VC. The data are expressed as the mean±SEM. n=5 per group. $^{*}P$<0.05, $^{**}P$<0.01 *vs* VC. $^{\#}P$<0.05, $^{\#\#}P$<0.01 *vs* ISO.

in the hearts of ISO-challenged mice pretreated with L7DG at 40 mg/kg bw. These results indicate that ISO increases the expression of NADPH oxidase subunits in the hearts and furthermore that L7DG pretreatment significantly suppresses ISO-induced expression of NADPH oxidase subunits in the heart.

L7DG prevents the heart from developing ISO-induced myocardial fibrotic lesions

Masson's trichrome staining visualizes collagen fibers and thus was used to evaluate fibrotic lesions in mice. As shown in Figure 4A and 4B, Masson's trichrome-stained interstitial collagen was observed in low abundance in the hearts of vehicle-treated normal controls, whereas a significantly increased amount of Masson's trichrome-stained collagen fibers was detected at the sites of microscopic injury in the hearts of ISO-challenged vehicle-treated mice. In distinct contrast, L7DG pretreatment resulted in a significant reduction in Masson's trichrome-stained areas in the heart. Collagen accumulation was also validated by Picrosirius red staining, and similar results were observed. As shown in Figure 4C and 4D, myocardial lesions were characterized by an overt increase in Picrosirius red-positive collagen deposition compared to that from vehicle-treated normal controls, which was significantly prevented by L7DG pretreatment. These results indicate that L7DG pretreatment prevents the heart from developing ISO-induced cardiac fibrosis.

α-Smooth muscle actin (α-SMA)-positive myofibroblasts are essential cellular executioners during the course of cardiac fibrogenesis[23]. The effect of L7DG pretreatment on preventing cardiac fibrosis was thus further confirmed by examining the expression of α-SMA in the heart. As shown in Figure 5A and 5B, α-SMA-expressing myofibroblasts were readily observed in ISO-challenged mouse hearts but were not encountered in the hearts from ISO-challenged mice pretreated with L7DG. The activity of TGFβ signaling, a major pathway involved in cardiac fibrosis[10], was also assessed by examining the expression of p-Smad2 in the mouse heart. As shown in Figure 6A and 6B, p-Smad2 immunoreactivity was readily detected and associated with myocardial injury in ISO-challenged vehicle-treated hearts, which was not observed in ISO-challenged mice pretreated with L7DG. Moreover, L7DG pretreatment was found to prevent ISO-induced increases in the mRNA levels of α-SMA, TGFβ and TGFβ receptor type 1 (TGFβRI) in the heart (Supplemental Figure 4). Additionally, the immunoreactivity of TGFβ1 was readily observed at the site of microscopic injury in the hearts of ISO-challenged vehicle-treated mice, which was not noted in ISO-challenged mice pretreated with L7DG at 40 mg/kg bw (Supplemental Figure 5). These results suggest that suppressed activity of TGFβ signaling is associated with the anti-fibrogenic effect of L7DG pretreatment.

L7DG pretreatment results in the downregulation of genes associated with fibrogenesis

Real-time PCR analyses of genes known to be involved in fibrogenesis were performed to understand the anti-fibrogenic effect of L7DG at a molecular level. As shown in Figure 7, collagen and non-collagen ECM genes were induced by ISO, and this induction was suppressed by L7DG pretreatment, which included Col1a1, Col1a2, Col3a1, Col12a1, Fbn1, elastin, and CTHRC1. Furthermore, increased expression of profibrogenic CTGF was observed in ISO-challenged hearts, whereas L7DG pretreatment resulted in significantly decreased expression of CTGF in the hearts of ISO-challenged mice. These results further validated the protective effects of L7DG against ISO-induced cardiac fibrosis.

L7DG pretreatment alters the expression of miRNAs implicated in fibrogenesis

To increase the understanding of pharmacological activity of L7DG against cardiac fibrosis, the expression of miRNAs asso-

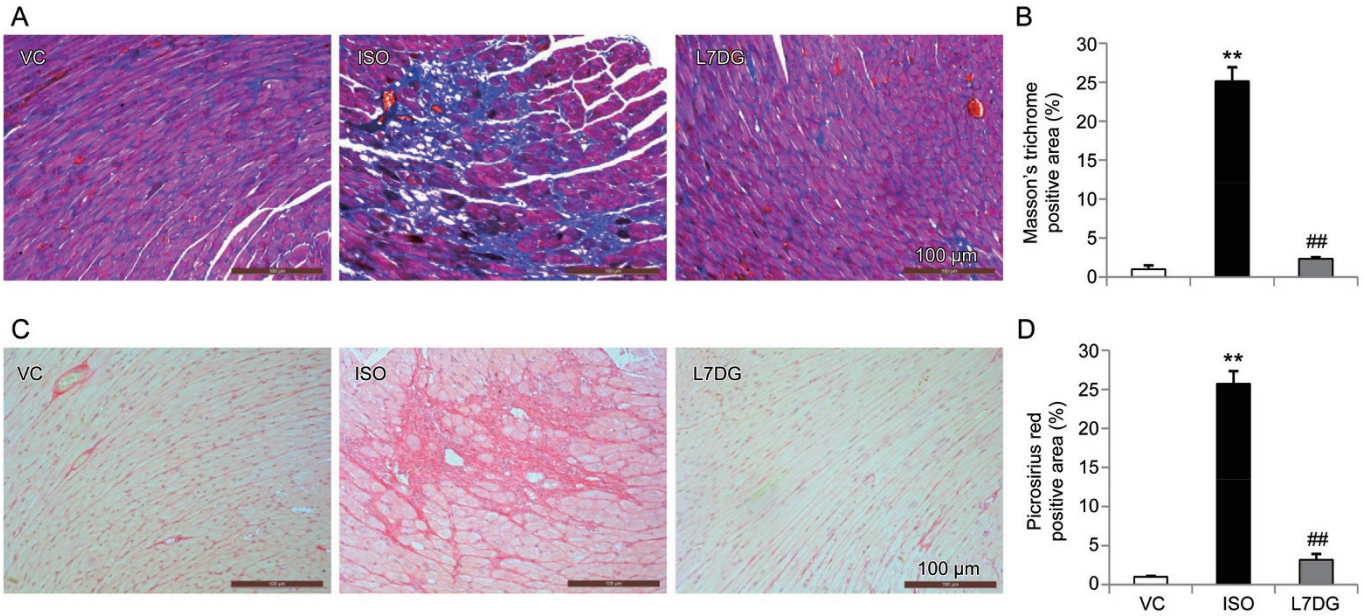

Figure 4. L7DG pretreatment prevented the heart from developing ISO-induced cardiac fibrosis. Masson's trichrome staining (A) or Picrosirius red staining (C) was performed on heart paraffin sections harvested from vehicle-treated normal controls (VC), ISO-challenged vehicle-treated mice (ISO), and ISO-challenged mice pretreated with L7DG at 40 mg/kg bw (L7DG). The percentage of Masson's trichrome-positive area per section (B) or that of Picrosirius red-positive area (D) was quantified. The data are expressed as the mean±SEM. *n*=4–6 per group. $^{**}P<0.01$ *vs* VC. $^{\#\#}P<0.01$ *vs* ISO.

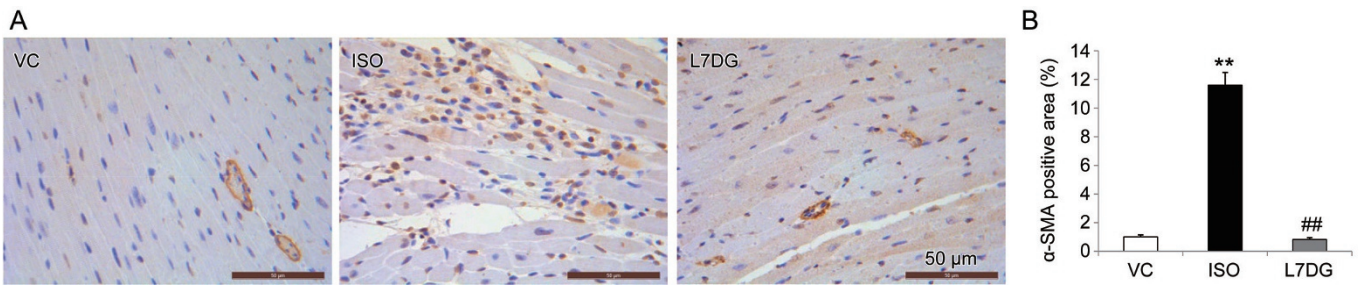

Figure 5. L7DG pretreatment decreased the expression of α-SMA in ISO-challenged hearts. (A) Cryosections were examined by IHC for the expression of α-SMA in the hearts collected from vehicle-treated normal controls (VC), ISO-challenged vehicle-treated mice (ISO), and ISO-challenged mice pretreated with L7DG at 40 mg/kg bw (L7DG). (B) The percentage of α-SMA-positive area per section excluding that of vessels was quantified. Scale bars: 50 μm. The data are expressed as the mean±SEM. *n*-4–6 per group. $^{**}P<0.01$ *vs* VC. $^{\#\#}P<0.01$ *vs* ISO.

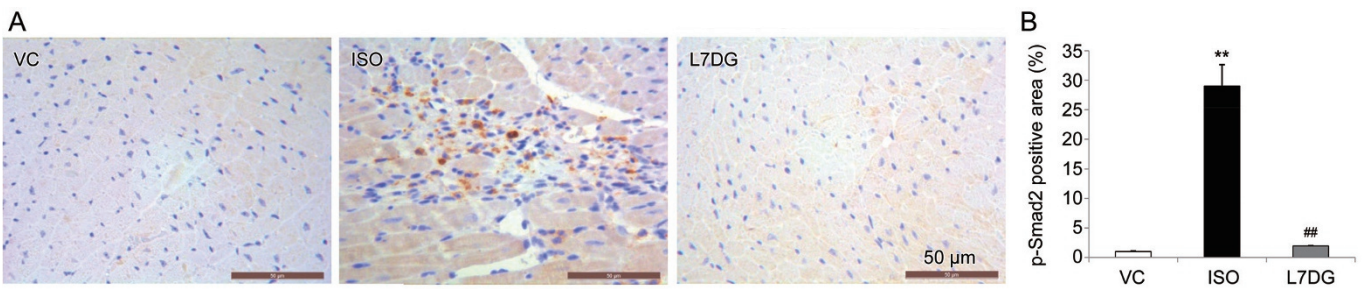

Figure 6. L7DG pretreatment decreased the level of p-Smad2 in ISO-challenged hearts. (A) The immunoreactivity of p-Smad2 was examined in the hearts collected from vehicle-treated normal controls (VC), ISO-challenged vehicle-treated mice (ISO), and ISO-challenged L7DG 40 mg/kg-treated mice (L7DG). (B) The percentage of p-Smad2-positive area was quantified. Scale bars: 50 μm. The data are expressed as the mean±SEM. *n*=4–6 per group. $^{**}P<0.01$ *vs* VC. $^{\#\#}P<0.01$ *vs* ISO.

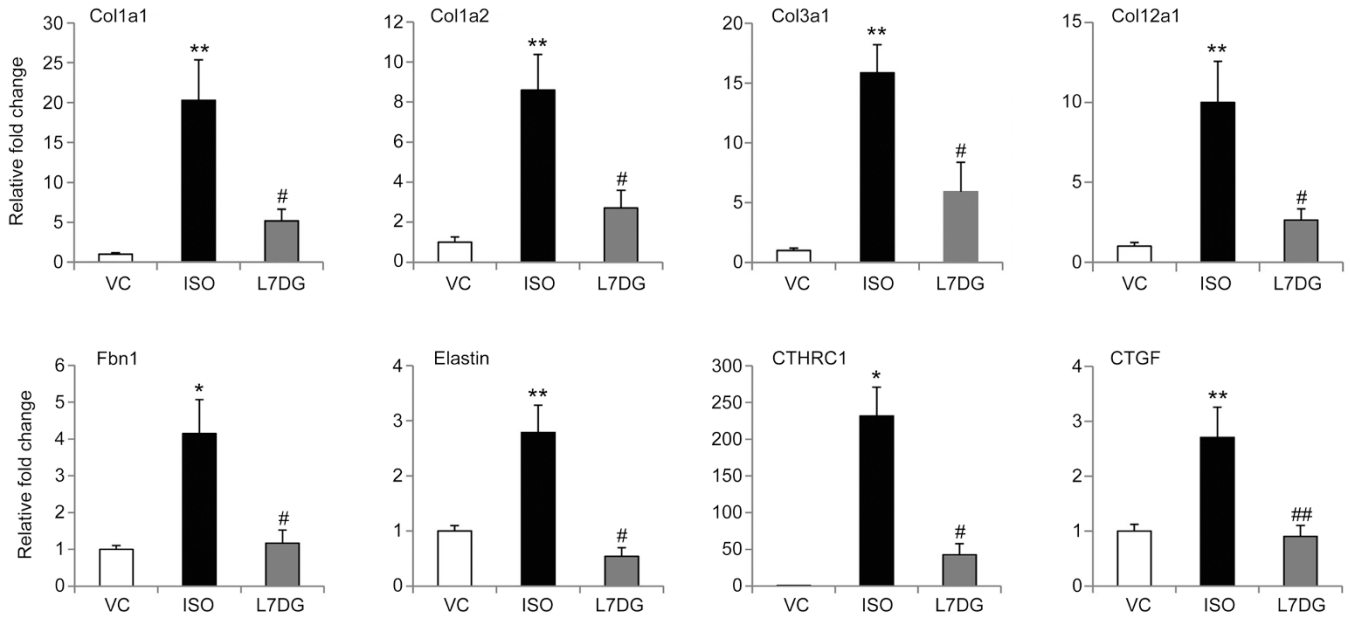

Figure 7. L7DG pretreatment suppressed ISO-induced cardiac expression of genes implicated in fibrogenesis. Total RNA was isolated from hearts collected from vehicle-treated normal controls (VC), ISO-challenged vehicle-treated mice (ISO), and ISO-challenged mice pretreated with L7DG at 40 mg/kg bw (L7DG). Real-time PCR was then performed to assess the relative expression of the indicated genes. The relative fold change in gene expression was plotted against that of VC. The data are expressed as the mean±SEM. n=5 per group. $^{**}P$<0.01 *vs* VC. $^{\#\#}P$<0.01 *vs* ISO.

ciated with fibrogenesis was analyzed. As shown in Figure 8, among six miRNAs examined, significantly increased expression of miR-21 and decreased expression of miR-29c-5p, miR-29c-5p, miR-30c-1-3p, and miR-30c-5p were observed in the hearts from ISO-challenged vehicle-treated mice compared to those observed in the normal controls. The expression

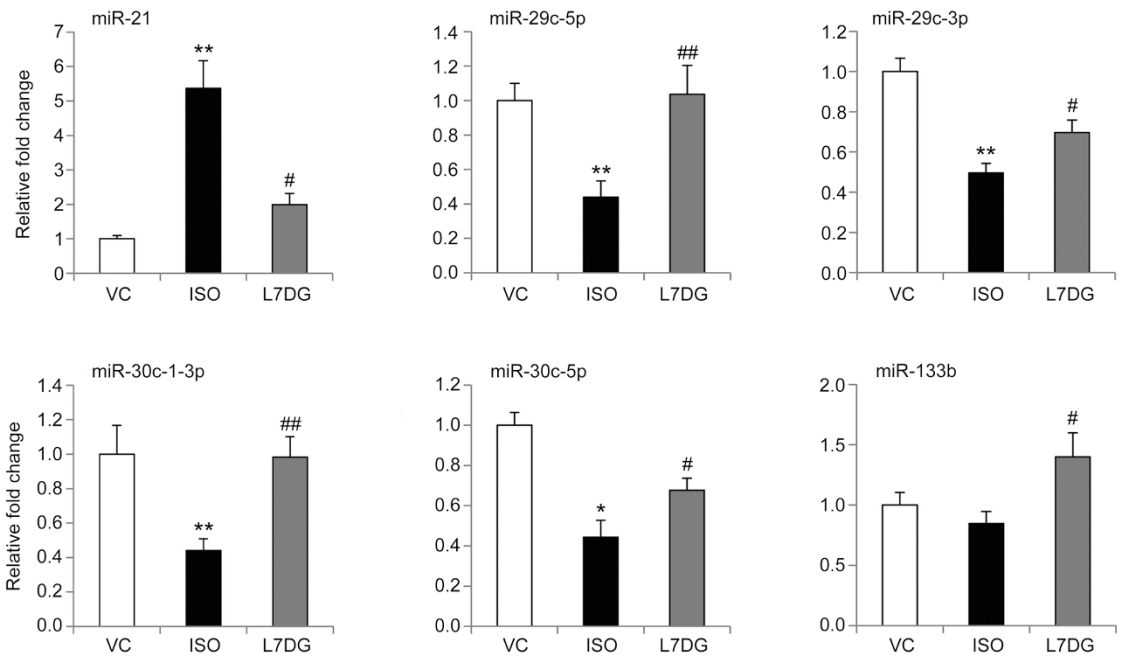

Figure 8. L7DG pretreatment resulted in altered levels of miRNAs implicated in fibrogenesis. Total RNA was isolated from paraffin sections encompassing the area marked by myocardial injury in ISO-challenged vehicle-treated mice (ISO) and the corresponding area in vehicle-treated normal controls (VC) and ISO-challenged mice pretreated with L7DG at 40 mg/kg bw (L7DG). Real-time PCR was then performed to assess the levels of indicated miRNAs. The relative fold change of each miRNA was plotted against that of the VC. The data are expressed as the mean±SEM. n=5 per group. $^{**}P$<0.01 *vs* VC. $^{\#}P$<0.05, $^{\#\#}P$<0.01 *vs* ISO.

level of miR-133b was not significantly changed in the hearts of ISO-challenged vehicle-treated mice. In contrast, L7DG pretreatment resulted in significantly decreased expression of miR-21 and increased expression of miR-29c-3p, miR-29c-5p, miR-30c-1-3p, and miR-30c-5p. Additionally, increased expression of miR-133b was observed in the hearts from ISO-challenged mice pretreated with L7DG. These results indicated that ISO challenge results in the dysregulated expression of miRNAs that regulate the expression of genes implicated in fibrogenic pathways. Moreover, significant changes in these miRNAs are associated with suppressed fibrosis as a result of L7DG pretreatment.

Table 3. L7DG attenuated ISO-induced myocardial injury.

Group	Histopathology score					
	–	+–	+	++	+++	*P* value
VC	5					
ISO				2	3	0.005
L7DG	2		1		1	0.02

L7DG posttreatment attenuates ISO-induced fibrosis

To further explore the therapeutic effects of L7DG on myocardial fibrosis, a posttreatment regimen was investigated (Supplemental Figure 1B). As shown in Figure 9A and Table 3, compared to those from the vehicle controls, ISO-challenged hearts were characterized by myocardial injury, and L7DG posttreatment resulted in significantly improved myocardial histology. Masson's trichrome staining and Picrosirius red staining were performed to examine and quantify collagen accumulation. Compared to that from the ISO-challenged vehicle-treated mice, L7DG posttreatment resulted in significantly attenuated collagen deposition as revealed by Masson's trichrome staining (Figure 9B and 9C) and Picrosirius red staining (Figure 9D and 9E), respectively. These results indicate that L7DG is therapeutically active in attenuating ISO-challenged myocardial fibrosis. Moreover, although better preserved myocardial histology was observed in ISO-challenged mice pretreated with L7DG compared to that from L7DG posttreatment regimen, no statistical significance was revealed by comparing the histopathology scores from two treatment regimens (Supplemental Table 2). A further comparison of Picrosirius red positivity revealed that compared to that from ISO-challenged mice pretreated with L7DG, an approximately 1.9-fold increase in Picrosirius red positivity was observed in the heart sections from ISO-challenged mice posttreated with L7DG (Supplemental Figure 6). Taken together, these results suggest that early administration of L7DG might result in better protection against ISO-induced myocardial injury.

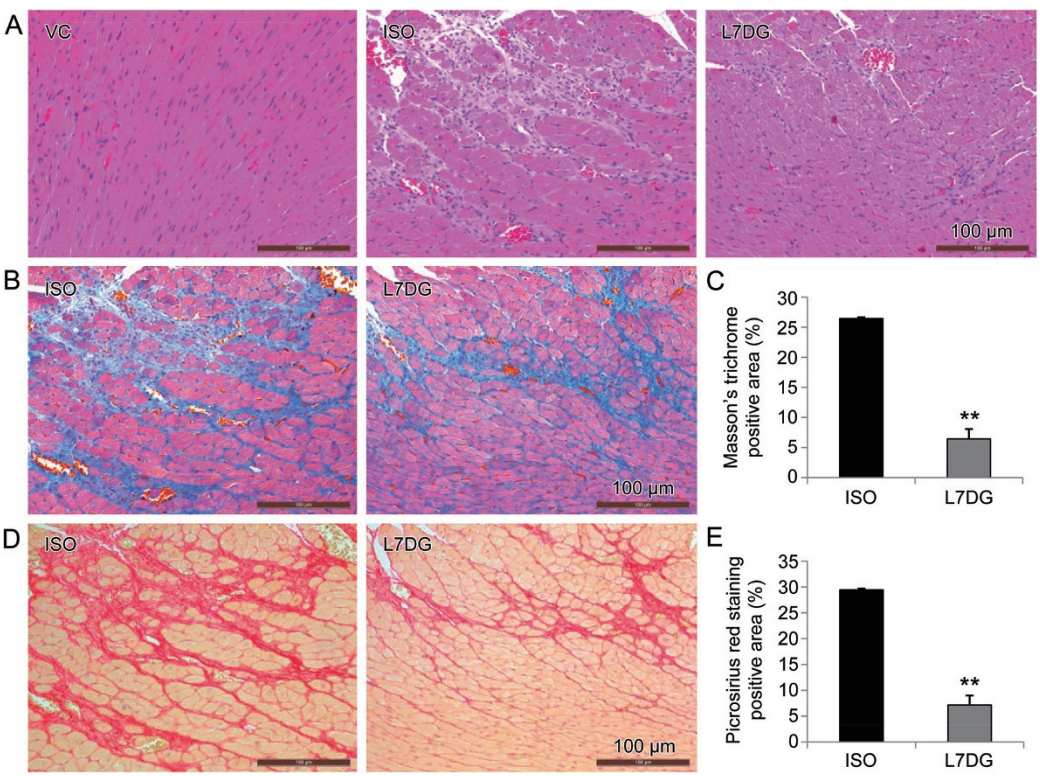

Figure 9. L7DG posttreatment alleviated ISO-induced myocardial injury in mice. H&E staining (A), Masson's trichrome staining (B) and Picrosirius red staining (D) were performed on the heart paraffin sections collected from vehicle-treated normal controls (VC), ISO-challenged vehicle-treated mice (ISO), and ISO-challenged mice treated with L7DG at 40 mg/kg bw (L7DG). The percentage of Masson's trichrome-positive area per section (C) or that of Picrosirius red staining (E) was quantified. Scale bar: 100 μm. The data are expressed as the mean±SEM. n=4–5 per group. $^{**}P<0.01$ *vs* ISO.

Discussion

The current study reveals the preventive and therapeutic effects of L7DG on ISO-induced myocardial injury and fibrosis. Morphological evidence shown here indicates that L7DG treatment resolves myocardial pathologies of myocardial granulation, inflammatory infiltration and fibrogenesis induced by ISO. At the molecular level, ISO-induced increases in the expression of genes implicated in oxidative stress and fibrogenesis were significantly suppressed by L7DG treatment. Furthermore, L7DG treatment alters the expression of miRNAs functioning as molecular fibrogenic modulators.

Administration of β adrenergic receptor agonist ISO results in cardiomyocyte necrosis, triggering myofibroblast proliferation and connective tissue accumulation[24]. NADPH oxidase is the primary enzymatic source of superoxide generation in mammalian cells[7]. The implication of NADPH oxidase-mediated oxidative stress in the pathogenesis of myocardial injury has been suggested by the observation of suppressed ROS generation in $p47^{phox}$-deficient mouse hearts during chronic myocardial infarction, implying that NADPH oxidase could be a therapeutic target for treating myocardial ischemic disorders[8]. Our previous study also demonstrated that apocynin, a naturally occurring NADPH oxidase inhibitor, prevents ISO-induced myocardial oxidative stress, morphological impairment and fibrogenesis in mice[9]. L7DG, which was previously suggested to be an antioxidant *in vitro*[14], was demonstrated here to alleviate ISO-induced injury and fibrosis in both preventive and therapeutic manners. Moreover, increased expression of genes encoding subunits of NADPH oxidase was observed in ISO-challenged mouse hearts. L7DG pretreatment, resulted in significantly decreased expression of these genes. These results indicate that the cardioprotective effects of L7DG may be due, in part, to suppression of ISO-induced upregulation of genes encoding NADPH oxidase. However, it remains to be further addressed in our future studies whether the protein levels of NADPH oxidase subunits, the activity of myocardial NADPH oxidase and the *in situ* production of ROS could be modulated by different L7DG treatment regimens in ISO-challenged hearts.

Cardiac fibrosis is an important pathological event characterized by myofibroblast activation and excessive ECM production. Elevated activity of TGFβ signaling is a crucial profibrogenic mechanism leading to myofibroblast activation and cardiac fibrosis[25]. L7DG pretreatment resulted in remarkable attenuation of the immunoreactivity of α-SMA and p-Smad2 in ISO-challenged hearts, verifying at a molecular level that L7DG treatment inhibited TGFβ signaling and myofibroblasts activation. Additional evidence corroborating the anti-fibrotic effect of L7DG was provided by decreased expression of ECM genes, including collagen- and collagen synthesis-related genes, which have been implicated in fibrosis formation in ISO-challenged L7DG-pretreated mouse hearts. These genes include those encoding predominant components of cardiac collagens, Col1a1 and Col3a1[26]. Col1a1 was increased by approximately 20.3-fold in ISO-challenged hearts compared to that from the vehicle-treated controls, whereas L7DG pretreatment reduced the expression of Col1a1 to approximately 5.2-fold of the vehicle-treated normal controls. A similar pattern was observed regarding the expression of Col3a1. An increase in Col3a1 expression by 15.9-fold was found in ISO-challenged hearts compared to that of vehicle-treated normal controls. L7DG pretreatment resulted in a significant reduction of Col3a1 expression to 5.9-fold of that detected in vehicle-treated normal controls. Moreover, L7DG pretreatment exhibited a striking effect on counteracting ISO-induced cardiac expression of non-collagen ECM genes, which included Fbn1[27] and elastin[28]. For instance, Fbn1 encodes a large, extracellular matrix glycoprotein that functions as a structural component of calcium-binding microfibrils. Fbn1 is abundantly expressed throughout the myocardium, highly inducible in response to fibrotic stimuli in fibroblasts and thus closely associated with reactive and reparative cardiac fibrosis. Fbn1 was induced to approximately 4.2-fold of that detected in vehicle-treated normal controls, whereas L7DG pretreatment led to decreased expression of Fbn1 to 1.2-fold of that detected in vehicle-treated normal controls. CTHRC1 can be induced by TGFβ[29], and in the vasculature, CTHRC1 has been identified to be induced in adventitial fibroblasts and neointimal SMCs and may contribute to the cellular response to artery injury[30]. In our study, ISO administration resulted in approximately 231.5-fold induction in the expression of CTHRC1, which decreased to 42.7-fold of that detected in vehicle-treated normal controls by L7DG pretreatment. CTGF is a secreted matricellular protein with profibrogenic properties and is often overexpressed in fibrotic lesions. CTGF is transcriptionally activated by TGFβ and plays central roles in mediating tissue fibrosis and remodeling through promoting cell adhesion, migration, angiogenesis, myofibroblast activation, and ECM deposition and remodeling. It has been reported that the inhibition of CTGF can reverse tissue fibrosis[31]. The cardiac expression of CTGF increased by 2.7-fold as a result of ISO challenge and decreased to 0.9-fold of that of the vehicle-treated normal controls by L7DG pretreatment. These results collectively provide molecular evidence supporting the anti-fibrotic effects of L7DG.

Moreover, it is worth noting that the cardioprotective effects of L7DG could very likely implicate miRNA-mediated expression regulation of multiple genes associated with TGFβ signaling (Figure 10). miRNAs have emerged as important regulators in various cellular and pathophysiological processes, including cardiac remodeling and fibrosis[13]. Accumulated evidence has demonstrated that the miR-29 family is implicated in fibrosis in multiple tissues, including the heart. An array of ECM genes have been identified as direct targets of miR-29 in fibroblasts, including collagens, fibrillins and elastin[32]. Moreover, miRNA-mediated gene expression regulation is tightly connected with TGFβ signaling during fibrogenic processes. TGFβ exerts modulatory effects on a number of miRNAs, including miR-21[33], miR-29[34], miR-30[35], and miR-133[36]. TGFβ induces the expression of miR-21, which has been demonstrated to be one of the most upregulated miRNAs induced by cardiac stress and is involved in cardiac fibrosis[37].

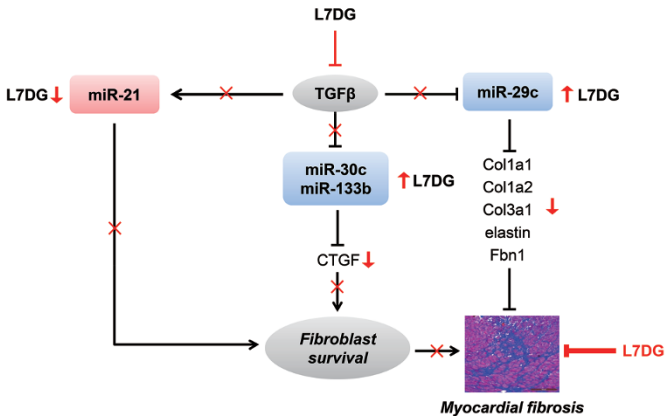

Figure 10. Cardioprotective effects of L7DG-implicated, TGFβ-associated, miRNA-mediated regulation of multiple genes. TGFβ signaling crosstalks with miRNA-regulated fibrogenic processes. TGFβ upregulates the expression of miR-21, a profibrogenic miRNA, and downregulates the expression levels of antifibrogenic miRNAs, including miR-29c, miR-30c, and miR-133b. Multiple genes encoding collagens, elastin, fibrillin 1 and CTGF are direct targets of miR-29c, miR-30c, and miR-133b, respectively. L7DG pretreatment resulted in decreased expression of miR-21 and increased expression of miR-29c, miR-30c, and miR-133b, which may in part contribute to attenuated myocardial fibrosis as a result of L7DG treatment through downregulation of collagens, elastin, fibrillin 1 and CTGF.

Downregulation of miR-21 has been considered a promising avenue to attenuate fibroblast proliferation, thus causing beneficial effects to the heart by inhibiting cardiac remodeling[38]. TGFβ also reduces the expression of miR-29, miR-30, and miR-133 families. Moreover, the expression of CTGF is under the regulation of miR-133 and miR-30 in the process of myocardial remodeling[39]. As revealed by the current study, the expression of miR-21 increased by approximately 5.4-fold in ISO-challenged mouse hearts compared to that in vehicle-treated normal controls; however, L7DG pretreatment significantly reduced the levels of miR-21 to approximately 2-fold of that detected in normal vehicle controls. As a result of ISO administration, the expression of miR-29c-3p and miR-29c-5p decreased to approximately 0.5 and 0.44-fold of that of the vehicle-treated normal controls, respectively. Decrease in the expression of miR-29 could enhance the fibrotic response by derepressing the expression of multiple collagens, fibrillins and elastin[32]. In contrast, in ISO-challenged L7DG-pretreated mice, the level of miR-29c-3p and miR-29c-5p significantly increased compared to that from ISO-challenged vehicle-treated mice, and furthermore, the level of miR-29-5p was nearly identical to that detected in vehicle-treated normal controls. Moreover, both miR-30c-1-3p and miR-30c-50 exhibited significant reduction in expression in ISO-challenged hearts, which was partially counteracted by L7DG pretreatment. It is also worth noting that although ISO did not result in significant changes in the level of miR-133b, it significantly increased in ISO-challenged L7DG-pretreated hearts.

It was noted that better protection against ISO-induced myocardial injury was achieved when L7DG was administered by a pretreatment regimen versus posttreatment regimen. These observations suggest that although L7DG was pharmacologically effective at protecting the heart when fibrogenic pathology was established, it may have a greater impact on the early events of ISO-induced myocardial injury. Future studies are thus required to further delineate the pharmacological mechanisms underlying the cardioprotective effects of L7DG.

In conclusion, our current study demonstrates for the first time that L7DG attenuates ISO-induced myocardial injury and fibrosis at both histopathological and molecular levels. Moreover, miRNAs-mediated gene expression regulation and its crosstalk with TGFβ signaling may in part be associated with the cardioprotective ability of L7DG against fibrosis. These results thus help increase the understanding of the pharmacological activities of L7DG and warrant further evaluation of L7DG as a promising cardioprotective agent.

Acknowledgements

This work was supported by the Program of Eastern Scholar at Shanghai Institutions of Higher Learning (Yu CHEN and Teng ZHANG), Shu Guang Project supported by Shanghai Municipal Education Commission (13SG42, Yu CHEN) and the National Natural Science Foundation of China (No 81273960, 81473732, Teng ZHANG and Yu CHEN).

Author contribution

Yu CHEN and Teng ZHANG conceived the project and designed experiments. Yu CHEN, Teng ZHANG, and Wei-liang ZHU analyzed the data and wrote the paper. Bing-bing NING, Yong ZHANG, Dan-dan WU, Li LIU, Jin-gang CUI, Pei-wei WANG, and Wen-jian WANG performed the experiments, analyzed the data and wrote part of the paper.

Supplementary information

Supplementary information is available at the website of Acta Pharmacologica Sinica.

References

1 Schaper J, Speiser B. The extracellular matrix in the failing human heart. Basic Res Cardiol 1992; 87: 303–9.
2 Whittaker P, Boughner DR, Kloner RA. Analysis of healing after myocardial infarction using polarized light microscopy. Am J Pathol 1989; 134: 879–93.
3 Kwong RY, Chan AK, Brown KA, Chan CW, Reynolds HG, Tsang S, *et al.* Impact of unrecognized myocardial scar detected by cardiac magnetic resonance imaging on event-free survival in patients presenting with signs or symptoms of coronary artery disease. Circulation 2006; 113: 2733–43.
4 Kwong RY, Sattar H, Wu H, Vorobiof G, Gandla V, Steel K, *et al.* Incidence and prognostic implication of unrecognized myocardial scar characterized by cardiac magnetic resonance in diabetic patients without clinical evidence of myocardial infarction. Circulation 2008; 118: 1011–20.
5 Assomull RG, Prasad SK, Lyne J, Smith G, Burman ED, Khan M, *et al.* Cardiovascular magnetic resonance, fibrosis, and prognosis in dilated cardiomyopathy. J Am Coll Cardiol 2006; 48: 1977–85.

6 Wattanapitayakul SK, Bauer JA. Oxidative pathways in cardiovascular disease: roles, mechanisms, and therapeutic implications. Pharmacol Ther 2001; 89: 187–206.
7 Lambeth JD. NOX enzymes and the biology of reactive oxygen. Nat Rev Immunol 2004; 4: 181–9.
8 Doerries C, Grote K, Hilfiker-Kleiner D, Luchtefeld M, Schaefer A, Holland SM, *et al*. Critical role of the NAD(P)H oxidase subunit p47phox for left ventricular remodeling/dysfunction and survival after myocardial infarction. Circ Res 2007; 100: 894–903.
9 Liu L, Cui J, Yang Q, Jia C, Xiong M, Ning B, *et al*. Apocynin attenuates isoproterenol-induced myocardial injury and fibrogenesis. Biochem Biophys Res Commun 2014; 449: 55–61.
10 Wipff PJ, Hinz B. Integrins and the activation of latent transforming growth factor beta1–an intimate relationship. Eur J Cell Biol 2008; 87: 601–15.
11 Fabian MR, Sonenberg N, Filipowicz W. Regulation of mRNA translation and stability by microRNAs. Annu Rev Biochem 2010; 79: 351–79.
12 Siomi H, Siomi MC. Posttranscriptional regulation of microRNA biogenesis in animals. Mol Cell 2010; 38: 323–32.
13 Thum T. Noncoding RNAs and myocardial fibrosis. Nat Rev Cardiol 2014; 11: 655–63.
14 Casanova E, Garcia-Mina JM, Calvo MI. Antioxidant and antifungal activity of *Verbena officinalis* L. leaves. Plant Foods Hum Nutr 2008; 63: 93–7.
15 Makino T, Ito M, Kiuchiu F, Ono T, Muso E, Honda G. Inhibitory effect of decoction of *Perilla frutescens* on cultured murine mesangial cell proliferation and quantitative analysis of its active constituents. Planta Med 2001; 67: 24–8.
16 Rona G, Chappel CI, Balazs T, Gaudry R. An infarct-like myocardial lesion and other toxic manifestations produced by isoproterenol in the rat. AMA Arch Pathol 1959; 67: 443–55.
17 Rona G. Catecholamine cardiotoxicity. J Mol Cell Cardiol 1985; 17: 291–306.
18 Teerlink JR, Pfeffer JM, Pfeffer MA. Progressive ventricular remodeling in response to diffuse isoproterenol-induced myocardial necrosis in rats. Circ Res 1994; 75: 105–13.
19 Zbinden G, Moe RA. Pharmacological studies on heart muscle lesions induced by isoproterenol. Ann N Y Acad Sci 1969; 156: 294–308.
20 Csapo Z, Dusek J, Rona G. Early alterations of the cardiac muscle cells in isoproterenol-induced necrosis. Arch Pathol 1972; 93: 356–65.
21 Kumar S, Enjamoori R, Jaiswal A, Ray R, Seth S, Maulik SK. Catecholamine-induced myocardial fibrosis and oxidative stress is attenuated by *Terminalia arjuna* (Roxb). J Pharm Pharmacol 2009; 61: 1529–36.
22 Purnomo Y, Piccart Y, Coenen T, Prihadi JS, Lijnen PJ. Oxidative stress and transforming growth factor-beta1-induced cardiac fibrosis. Cardiovasc Hematol Disord Drug Targets 2013; 13: 165–72.
23 Turner NA, Porter KE. Function and fate of myofibroblasts after myocardial infarction. Fibrogenesis Tissue Repair 2013; 6: 5.
24 Benjamin IJ, Jalil JE, Tan LB, Cho K, Weber KT, Clark WA. Isoproterenol-induced myocardial fibrosis in relation to myocyte necrosis. Circ Res 1989; 65: 657–70.
25 Ueha S, Shand FH, Matsushima K. Cellular and molecular mechanisms of chronic inflammation-associated organ fibrosis. Front Immunol 2012; 3: 71.
26 Fan D, Takawale A, Lee J, Kassiri Z. Cardiac fibroblasts, fibrosis and extracellular matrix remodeling in heart disease. Fibrogenesis Tissue Repair 2012; 5: 15.
27 Bouzeghrane F, Reinhardt DP, Reudelhuber TL, Thibault G. Enhanced expression of fibrillin-1, a constituent of the myocardial extracellular matrix in fibrosis. Am J Physiol Heart Circ Physiol 2005; 289: H982–91.
28 Teekakirikul P, Eminaga S, Toka O, Alcalai R, Wang L, Wakimoto H, *et al*. Cardiac fibrosis in mice with hypertrophic cardiomyopathy is mediated by non-myocyte proliferation and requires TGF-beta. J Clin Invest 2010; 120: 3520–9.
29 Bauer Y, Tedrow J, de Bernard S, Birker-Robaczewska M, Gibson KF, Guardela BJ, *et al*. A novel genomic signature with translational significance for human idiopathic pulmonary fibrosis. Am J Respir Cell Mol Biol 2015; 52: 217–31.
30 LeClair RJ, Durmus T, Wang Q, Pyagay P, Terzic A, Lindner V. Cthrc1 is a novel inhibitor of transforming growth factor-beta signaling and neointimal lesion formation. Circ Res 2007; 100: 826–33.
31 Lipson KE, Wong C, Teng Y, Spong S. CTGF is a central mediator of tissue remodeling and fibrosis and its inhibition can reverse the process of fibrosis. Fibrogenesis Tissue Repair 2012; 5: S24.
32 van Rooij E, Sutherland LB, Thatcher JE, DiMaio JM, Naseem RH, Marshall WS, *et al*. Dysregulation of microRNAs after myocardial infarction reveals a role of miR-29 in cardiac fibrosis. Proc Natl Acad Sci U S A 2008; 105: 13027–32.
33 Kumarswamy R, Volkmann I, Jazbutyte V, Dangwal S, Park DH, Thum T. Transforming growth factor-beta-induced endothelial-to-mesenchymal transition is partly mediated by microRNA-21. Arterioscler Thromb Vasc Biol 2012; 32: 361–9.
34 Wang J, Wang Y, Ma Y, Lan Y, Yang X. Transforming growth factor beta-regulated microRNA-29a promotes angiogenesis through targeting the phosphatase and tensin homolog in endothelium. J Biol Chem 2013; 288: 10418–26.
35 Volkmann I, Kumarswamy R, Pfaff N, Fiedler J, Dangwal S, Holzmann A, *et al*. MicroRNA-mediated epigenetic silencing of sirtuin1 contributes to impaired angiogenic responses. Circ Res 2013; 113: 997–1003.
36 Duan LJ, Qi J, Kong XJ, Huang T, Qian XQ, Xu D, *et al*. MiR-133 modulates TGF-beta1-induced bladder smooth muscle cell hypertrophic and fibrotic response: implication for a role of microRNA in bladder wall remodeling caused by bladder outlet obstruction. Cell Signal 2015; 27: 215–27.
37 van Rooij E, Sutherland LB, Liu N, Williams AH, McAnally J, Gerard RD, *et al*. A signature pattern of stress-responsive microRNAs that can evoke cardiac hypertrophy and heart failure. Proc Natl Acad Sci U S A 2006; 103: 18255–60.
38 van Rooij E, Olson EN. Searching for miR-acles in cardiac fibrosis. Circ Res 2009; 104: 138–40.
39 Duisters RF, Tijsen AJ, Schroen B, Leenders JJ, Lentink V, van der Made I, *et al*. miR-133 and miR-30 regulate connective tissue growth factor: implications for a role of microRNAs in myocardial matrix remodeling. Circ Res 2009; 104: 170–8.